

Calculation of Aircraft Target's Single-Pulse Detection Probability

Kuizhi Yue^{1,2}, Shichun Chen², Changyong Shu²

ABSTRACT: The original radar cross section data or some rough models are often used to estimate a given aircraft target detection probability. The calculation results may not be very accurate as targets are different from one another and the real radar detection process is complex. A new method for radar cross section model generation is proposed and it takes the random factors like air turbulence into account; this makes it conform to the reality. In addition, this radar cross section model can be directly applied to the radar detection process to calculate the detection probability of a specific aircraft at any attitude. Four typical aerial vehicles are taken as examples to demonstrate this method and information such as detection probability, signal to noise ratio and detection distance. Target's instantaneous probability of being tracked, which corresponds to target's detection probability, can also be calculated. Using these calculation results, we can compare two different aircrafts' stealth performance in detail or optimize an aircraft's flight path.

KEYWORDS: Detection probability, RCS fluctuation, Stealth performance, Aircraft target.

INTRODUCTION

It is a common practice that a radar cross section (RCS) of a target is interpreted as the target's stealth performance or its detection probability by hostile radar. We all know that an aircraft with RCS value of $\sigma = 0.1 \text{ m}^2$ sounds better than one with $\sigma = 1 \text{ m}^2$, but nobody can promise us that the first performs better than the latter in front of a really working radar, as radar detection process is probabilistic. The detection probability is influenced by many random factors, such as the radar system's parameters, the natural environment and most of all, as well as the RCS fluctuation characteristic of the target.

Radar system designers have utilized RCS fluctuation models to indicate a certain kind of targets for a long time. Plenty of researching work has been done and classical models like Swerling models, chi-square models etc. have been widely used (Shnidman 1995, 2005; Swerling 1960; Scholefield 1967). But all these models are meant to estimate a radar system's detecting performance, not the stealth performance of an aircraft target. If those models are directly used on a specific aircraft, the process is somehow tedious and may cause great errors in model building (Johnston 1997).

However, we definitely need to know the detection probability of a specific aircraft. RCS is the fundamental parameter of an aircraft, whereas the detection probability is a parameter more important and intuitive. In a real combat situation, detection probability, along with target's RCS fluctuation characteristic, radar detection distance, false alarm probability, signal to noise ratio (SNR) etc. should all be taken into consideration. These parameters can give us a more objective evaluation on the stealth performance of a specific aircraft. Researchers studying the optimal path planning for aerial vehicles are the representative ones who

1.Naval Aeronautical and Astronautical University – Department of Airborne Vehicle Engineering – Yantai – China. **2.**Beihang University – School of Aeronautic Science and Engineering – Beijing – China.

Author for correspondence: Shichun Chen – Beihang University – School of Aeronautic Science and Engineering – Beijing 100191 – China | Email: 36050225csc@sina.com

Received: 02/16/2015 | **Accepted:** 06/16/2015

care about real combat situations. When optimizing aircraft's flight path in a radar threatening situation, they need to know the stealth performance of the aircraft, as accurately as possible.

A lot of literature about path planning has been published. The early studies always treat the threatening radar as obstacles (Goerzen and Mettler 2010; Xu *et al.* 2010), which means the target's detection probability is either 0 or 100%. Some researchers proposed aircraft's dynamic RCS models which deal with RCS both in azimuth and bank angles (Moore 2002; Bortoff 2000; Hebert 2001; Kim and Bang 2007), but they did not give any analysis on detection probability. Dogan (2003) and Wu *et al.* (2011) used probabilistic map to estimate the detection probability; the map is defined as the risk of exposure to the radar threats. And the risk is a function of target's position. But this map is rough and cannot represent a specific target accurately. Misovec *et al.* (2003) and Inanc and Muezzinoglu (2008) built a detection model using two different tables, which contain some parameters about the aircraft as well as the radar system. They also gave an approximation function to express the detection probability. Parameters in both tables are also very general and only represent a certain kind of targets; when dealing with a specific aircraft, they may bring unexpected errors.

A popular model for calculating the target's detection probability was firstly proposed in Zeitz's doctoral dissertation (Zeitz 2005). He derived an approximation function of target's instantaneous probability of being tracked. Many researchers prefer to use his function to calculate the aircraft's probability of being tracked and then optimize the aircraft's flight path based on the calculation results (Ding *et al.* 2008; Liu *et al.* 2012; Mo *et al.* 2014; Kabamba *et al.* 2006). This function considers many variables such as target's RCS values, false alarm probability, SNR and radar system's working settings. It also has a precise approximation expression, so it can give an accurate detection probability for any given RCS data.

The purpose of this paper is not to develop a new or improve an old path planning method. We focus on the aircraft's stealth performance evaluation, from the perspective of detection probability. The calculation results will be useful if we want to know a specific aircraft's stealth performance in a real combat situation, and they can also be used in path planning optimizations.

SINGLE-PULSE DETECTION PROBABILITY OF RCS FLUCTUATING ZEITZ'S FUNCTION

As Zeitz's function is efficient in detection probability calculation and is widely used in estimating aircraft's stealth

performance, we will analyze his function in this subsection. The first variable in his function is the SNR, as defined in Eq. 1:

$$S_r(\sigma, R) = \frac{K\sigma}{R^4} \quad (1)$$

where:

S_r is SNR; σ is target's RCS; R is the distance between radar and target; and K is a constant indicating radar system's processing ability.

In fact, this equation is the derivation of the basic radar equation and no probabilistic variable is involved here.

The second variable is the detection probability, P_D , expressed as a function of SNR and false alarm probability, P_{fa} , as shown in Fig. 1 (Zeitz 2005).

This figure actually shows the single pulse detection probability of a signal with unknown phase but known amplitude (Difanco and Rubin 1968). The analytical expression of P_D can be written as:

$$P_D = \int_{r_b}^{\infty} r \exp\left(-\frac{r^2 + S_r}{2}\right) I_0(r\sqrt{S_r}) dr \quad (2)$$

where:

r_b is the detection threshold; r is an intermediate variable; S_r is SNR; and I_0 is the modified Bessel function of the first kind and order zero.

The SNR here can be expressed as Eq. 3 and it has no matter with Eq. 1.

$$S_r = \frac{2E}{N_0} \quad (3)$$

where:

E is the signal energy and $N_0/2$ is the two-sided white Gaussian noise spectral density. S_r here is equal to the ratio of maximum instantaneous signal power to average noise power out of a matched filter (Difanco and Rubin 1968), and SNR in Zeitz (2005) is equal to the ratio of average instantaneous power to average noise power. So there exists a 3 dB discrepancy between figures drawn by Eq. 2 and Fig. 1, when P_{fa} value keeps the same.

Then a probability of track loss, $z[n]$, is defined as a recursion expression:

$$z[n+1] = (1 - z[n-l])P_D(P_m)^l + z[n] \quad (4)$$

where:

n is the transmitting pulses number and l is the consecutive misses number, being $n > l$ and $l > 2$; P_m is the missing probability, being $P_m = 1 - P_D$.

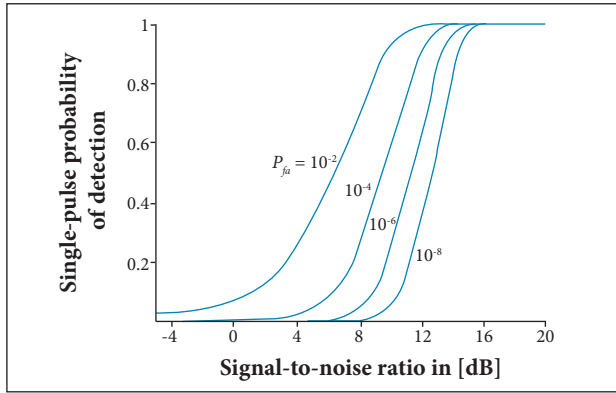


Figure 1. Detection probability versus SNR and false alarm probability.

The instantaneous probability of being tracked, P_{track} , can then be expressed as Eq. 5 and its approximation function can be expressed as Eq. 6. The average probability of being tracked during a time interval, ΔT , can be expressed as Eq. 7.

$$P_{track} = 1 - z[n] \tag{5}$$

$$P_{track}(\sigma, R) = \frac{1}{1 + \left(\frac{c_2 R^4}{\sigma}\right)^{c_1}} \tag{6}$$

$$\overline{P_{track}} = \frac{1}{\Delta T} \int_{t-\Delta T}^t P_{track}(\tau) d\tau \tag{7}$$

where:

c_1 and c_2 are radar constants; t is time; τ is the time increment.

Equations 4 and 5 combine P_{track} and P_D . Equation 6 uses Eq. 1 as its SNR variable to connect P_{track} , R and σ , though the theoretical SNR should be Eq. 3. This substitution of SNR may cause extra calculation error.

P_D in Eq. 2 is derived on assumption that the amplitude of the signal to be detected is already known, which means the target's RCS value is a known constant in this equation, and no matter how many pulses are transmitted, the back scattering pulses will keep the same amplitude. This assumption does not take the RCS fluctuation characteristic into account, which may bring some errors in P_D calculation and in the following P_{track} calculation.

BASIC STEPS OF DETECTION PROBABILITY CALCULATION

A simplified optimum detector for a single pulse of known amplitude and unknown phase can be illustrated in Fig. 2 (Difanco and Rubin 1968).

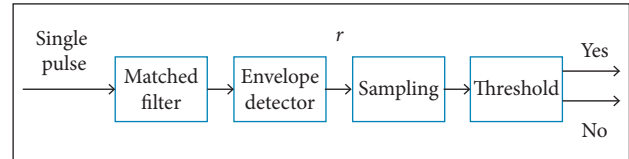


Figure 2. Optimum detector for a single pulse.

When the target is absent, the probability density function (PDF) of the intermediate variable, r , can be expressed as Eq. 8. This intermediate variable, r , is the output of a typical radar receiver's envelope detector.

$$p(r) = r \exp\left(-\frac{r^2}{2}\right) \tag{8}$$

And, according to its definition, the false alarm probability can be expressed as:

$$P_{fa} = \int_{r_b}^{\infty} r \exp\left(-\frac{r^2}{2}\right) dr = \exp\left(-\frac{r_b^2}{2}\right) \tag{9}$$

If the P_{fa} value is given, the threshold can be solved by Eq. (9) and expressed as:

$$r_b = \sqrt{2 \ln \frac{1}{P_{fa}}} \tag{10}$$

When the target is present, the PDF of r can be expressed as:

$$p(r) = r \exp\left(-\frac{r^2 + S_r}{2}\right) I_0(r\sqrt{S_r}) \tag{11}$$

Then the detection probability, P_D , can be expressed as Eq. 2. When target's RCS fluctuation characteristic is taken into consideration, the amplitude of the back scattering pulse changes with RCS. Equation 2 should be averaged with respect to amplitude statistics as:

$$P_D = \int_0^{\infty} \int_b^{\infty} r \exp\left(-\frac{r^2 + S_r}{2}\right) I_0(r\sqrt{S_r}) \cdot p(A) dr dA \tag{12}$$

where;

A is the back scattering pulse amplitude; $p(A)$ is the PDF of A .

When the RCS data of the aircraft target is known, $p(A)$ can be obtained using the simple Eq. 13:

$$\sigma = a \cdot A^2 \tag{13}$$

where:

a is a constant depending on radar system's working parameters, such as transmitting power, antenna gain etc., and the distance R .

Radar experts prefer to use a fluctuation model, like a Swerling model, in Eq. 12 to estimate the radar system's detecting performance when facing a "Swerling" target. If we want to know a specific aircraft's detection probability, we can directly use the discrete RCS data of the aircraft to generate a $p(A)$ and substitute it into Eq. 12 to obtain target's single pulse detection probability. This method can give a more accurate P_D .

DETECTION PROBABILITY OF A SPECIFIC AIRCRAFT TARGET'S RCS MODEL GENERATION

When radar experts use classical fluctuation models to analyze radar system's performance, they do not need to know the exact attitude domain of the target. When aerospace experts use approximation models to analyze a specific aircraft's detection probability, they always assume that every attitude angle of the target has an equal probability of being presented to the radar (Robinson 1992; David 2007). This assumption is not always the reality and will bring some trouble in P_D calculation accuracy.

Our purpose is to calculate the P_D of a specific aircraft at a given angle θ_0 . We need to know the RCS value corresponding to that given angle as well as other RCS values around that angle, because an aircraft in flight will always experience turbulence and other micro motions, and target's RCS varies dramatically even with a small change in attitude (Paterson 1999). Taking into account these random factors, we assume that these RCS values obey the normal distribution when presented to the radar.

When the aircraft is cruising, the elevation angle between target and radar does not change as much as the azimuth angle, and the RCS in this small elevation angle domain varies not so dramatically as it does in the azimuth angle domain. For simplicity, we only analyze RCS data in azimuth angle. The

method described here can also be applied to RCS data obtained both in azimuth and elevation angles.

Figure 3 shows the framework of target's RCS model generation: σ_0 of the original RCS data corresponds to the azimuth angle θ_0 ; σ_i ($i = 1, 2, \dots, m$) corresponds to an azimuth angle θ_i ; θ_i is from an azimuth angle domain, $\theta_0 - \Psi \sim \theta_0 + \Psi$, whose center is at θ_0 , and θ_i is different from θ_0 ; $m + 1$ is the total number of RCS values in this angle domain. This domain should be small enough if the aircraft flies relatively steadily. It is intentionally exaggeratedly drawn in Fig. 3 just for convenience.

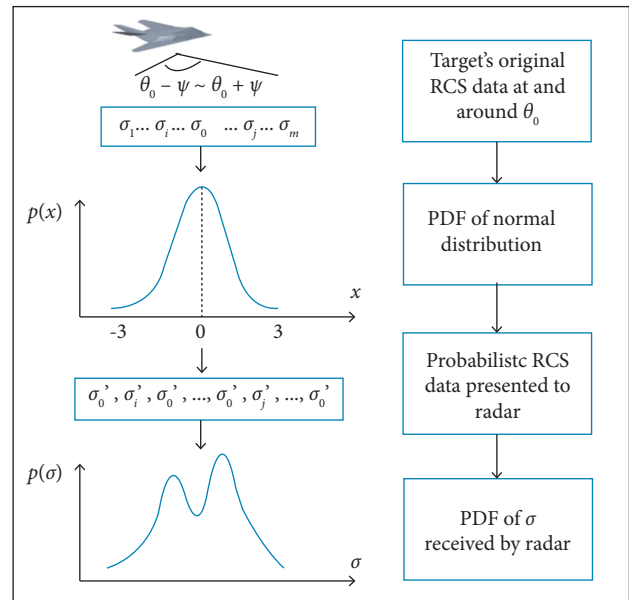


Figure 3. Framework of RCS model generation.

The normal distribution in Fig. 3 is the one-dimensional normal distribution. The expectation value of x in the normal distribution is set to be 0, and the standard deviation is set to be 1. Both set values will not influence the calculation results because what matters is the probability value of x , not the value of x itself. So the distribution can be expressed as:

$$p(x) = \frac{1}{\sqrt{2\pi}} \exp\left(-\frac{x^2}{2}\right), -3 < x < 3 \tag{14}$$

Equation 14 can be used to generate a series of random values of x . Each x value corresponds to a specific angle value and, consequently, a specific RCS value. The range of x in Eq. 14 is limited to be $-3 \sim 3$ because $p(x)$ decreases to nearly 0 beyond $x = \pm 3$. So the curve of $p(x)$ can be truncated at $x = \pm 3$; this means $x = \pm 3$ exactly corresponds to the two extremes of the

azimuth angle domain, respectively. The extremes are set to be θ_1 and θ_m , and their corresponding RCS values are σ_1 and σ_m .

The “normrnd” function of MATLAB can be used to conduct this random process and generate a series of x values which obey the normal distribution. Using these x values, a series of RCS values can be obtained from the corresponding angle domain, as shown in the third frame of Fig. 3. These probabilistic RCS values presented to the radar are much different from the original one. σ_0 may appear much more times than σ_i . And the PDF of these random RCS values is different from that of the original ones. This PDF can then be used to calculate P_D .

The variable presented in Fig. 3 is σ ; when applied to numerical calculation, the variable A is preferred, the derivation is the same as that of σ , and Eq. 13 can be used to obtain $p(A)$ conveniently.

NUMERICAL CALCULATIONS AND ANALYSIS

In order to demonstrate our method, we choose four different types of aerial vehicles and obtain their RCS data by self-programmed software which is based on the physical optics (PO), equivalent current method (ECM), physical theory of diffraction (PTD) and shooting and bouncing ray method (SBR). There are unavoidable errors in the RCS simulation results and we can never know the real RCS of a real aircraft like F-117A. However, our purpose is not to get an accurate RCS value of a target; we care more about target’s RCS fluctuation characteristic and this self-programmed software can give a satisfactory prediction about target’s RCS fluctuation trend.

Figure 4 shows the RCS calculation mockups. SDM means self-designed missile. It is just an imaginary one and can be classified as a stealth vehicle like F-117A as it obeys the basic stealth designing principles. X-21 is a big and conventional aircraft manufactured by Northrop and F-16 is a small and conventional aircraft.

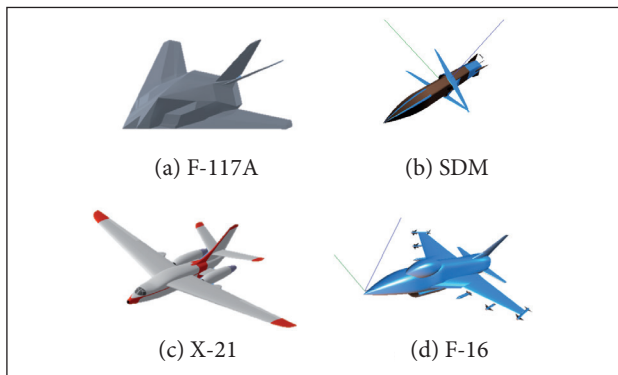


Figure 4. RCS calculation mockups.

RCS calculation is conducted at L band, which is often used in ground-based searching radars (Paterson 1999). The polarization direction is horizontal. The calculation angle interval is 0.1° . The azimuth angle domain is set to be $\theta_0 - 3^\circ \sim \theta_0 + 3^\circ$.

Figure 5 shows the RCS values of these four targets. $\theta = 0^\circ$ corresponds to each target’s head direction. We can see that F-117A and SDM have comparably small RCS values; most of their RCS values are smaller than 0 dB.m^2 . X-21 and F-16 have higher RCS values; most of their RCS values are much higher than 0 dB.m^2 . Figure 5 cannot tell us the specific detection probability, method mentioned in the previous sections can be used to obtain a specific detection probability.

Firstly, Monte-Carlo (MC) method is used to generate the PDF of the back scattering pulse’s amplitude. The first step is to generate a series of random values using “normrnd” function,

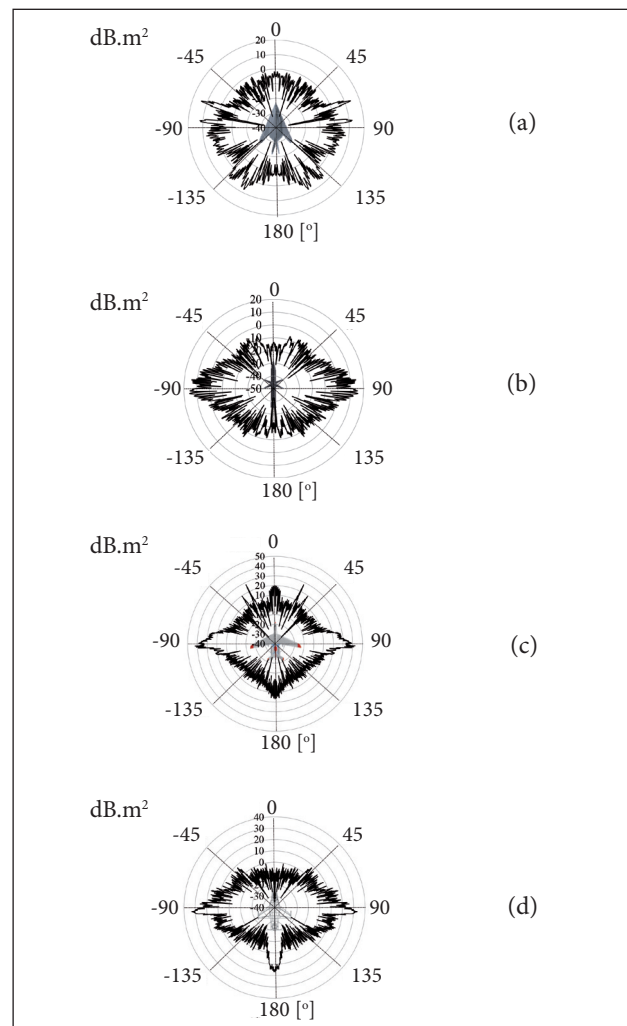


Figure 5. Targets’ RCS polar curves. (a) F-117A; (b) SDM; (c) X-21; (d) F-16.

as described in the previous section. This function should be run enough times to generate enough x values to cover the whole range of $-3 \sim 3$ and, consequently, the whole range of $\theta_0 - 3^\circ \sim \theta_0 + 3^\circ$. We have conducted a lot of calculations, and the empirical repeating times for “normrnd” function is about 10,000 ~ 15,000. Then a steady PDF of these RCS values can be obtained, and this PDF can be used in Eq. 12 to obtain PD corresponding to the azimuth angle of θ_0 .

Figure 6 shows the influence of repeating times, N , on the PDF curve's steadiness. E_r indicates the difference between the PDF of $N = 20,000$ and the PDF when $N \neq 20,000$. It is shown that when N exceeds about 10,000, the difference between 2 PDF curves is very small. The RCS data used here is from the azimuth angle domain $64^\circ \sim 70^\circ$ of F-117A, but the conclusion is correct when the target or angle domain changes. E_r is defined in Eq. 15:

$$E_r = \sum_{i=1}^k [p_N(i) - p_0(i)]^2 \quad (15)$$

where:

p_N is the PDF when $N \neq 20,000$; p_0 is the PDF when $N = 20,000$; i ($i = 1, 2, \dots, k$) indicates the discrete point of the PDF curve.

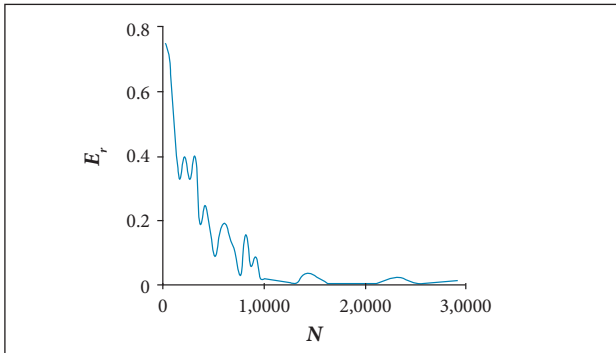


Figure 6. Influence of N on the PDF curve's steadiness [data from F-117A].

When the random process is conducted, the PDF of the back scattering values may be very different from the original one. Figure 7 shows the PDF of RCS from the angle domain of $64^\circ \sim 70^\circ$ of F-117A. The solid line indicates PDF after conducting random process on the original data and the dotted line indicates PDF without random process, which means every RCS value in the original data have an equal probability to be presented to the radar. Two PDF curves are different either in configuration or

in RCS data range. This will lead to a difference in P_D values. In this case, when the random process is considered, the result is $P_D = 0.45$ and when random process is not considered, $P_D = 0.53$. SNR is about 14 dB and false alarm probability $P_{fa} = 10^{-6}$, for both cases. If $P_D = 0.50$ is the threshold to declare a single pulse detection, these 2 PDFs will bring different conclusions.

Figure 8 shows the relationship between SNR and P_D for the conventional target X-21 and the stealth missile SDM. $\theta = 0^\circ$ corresponds to the head direction. P_D generally changes with SNR. The P_D of X-21 can always exceed 0.5 in the head direction, normal direction of leading edge, fuselage side direction and tail direction. In other directions, its P_D is very small. As to SDM, its P_D can always keep an even smaller

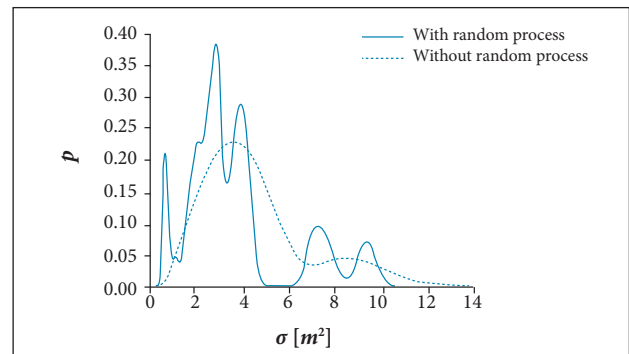


Figure 7. PDFs of F-117A at $\theta_0 = 67^\circ$, with and without random process.

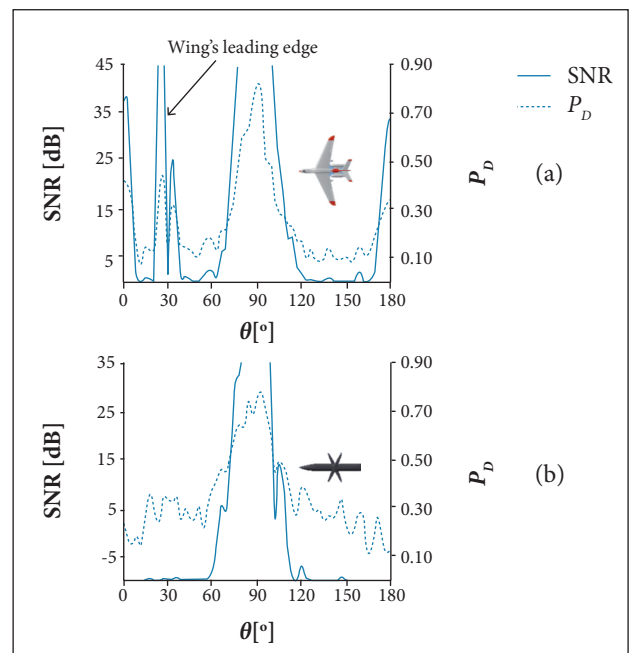


Figure 8. Relationship between SNR and P_D ($P_{fa} = 10^{-6}$). (a) X-21; (b) SDM.

value at all angles except those near the side direction. Radar working parameters for both vehicles are the same and the normalized detection distance of X-21 is twice that of SDM. If the working parameters of hostile radar are known, we can calculate target's detection probability at any given distance and we are able to obtain the exact values of P_D , SNR, P_{fa} and R . We can also compare two different targets' stealth performance in the same threatening situation. The calculation results can help a lot on optimizing a flight path.

For a specific target, if more data about P_D , SNR, P_{fa} and R are obtained, a complex polar curve can be drawn. Figure 9 gives an example for the stealth aircraft F-117A and conventional aircraft F-16. For each target, the radar is set to be at three different distances, with some certain working parameters. The detection distance R is normalized here because SNR varies with detection distance as well as radar transmitting power, radar antenna gain etc. If the transmitting power here is 200 W, the antenna gain is 30 dB, and other loss factors are set as common values; 1.0 R is about 15 km and the average SNR is about 15 ~ 20 dB. If the working parameters change, P_D will change but the configuration and trend of its curve will not change too much.

Figure 9(a) shows that F-117A performs well in the direction between about $\theta = 0^\circ \pm 60^\circ$. This is an important angle domain to

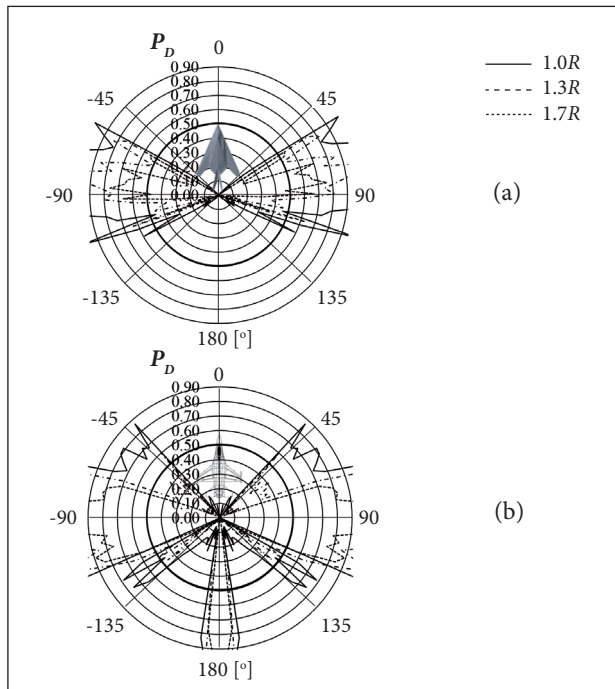


Figure 9. Target's azimuth detection probability at different distances ($P_{fa} = 10^{-6}$). (a) F-117A; (b) F-16.

a military aircraft. It also performs well in its tail direction between about $\theta = 180^\circ \pm 65^\circ$. P_D in both domains is much smaller than 0.5 and the target can be regarded as perfectly stealthy. In the side direction between about 60° to 115° , F-117A performs not so well, P_D can always exceed 0.5, but if the detection distance increases (so SNR decreases), P_D will decrease fast synchronously in the whole angle domain.

Figure 9(b) shows that F-16 has a very low P_D in the direction between about $\theta = 0^\circ \pm 40^\circ$. This sounds good but may not be the reality because the RCS calculation mockup of F-16 assumes that its cockpit and radar cabin have smooth surfaces from the perspective of electromagnetic. And RCS of its inlet may not be calculated accurately because of mockup's simplification. In fact, the real F-16 fighter plane does not have these smooth surfaces, cockpit and radar cabin are just 2 strongest RCS scatters on it. P_D in the tail direction is big because F-16's nozzle does not have any stealth optimization measures. In the side direction between about 40° , which is just the normal direction of its wing's leading edge, and 135° , F-16 has a very big P_D , and if the detection distance increases (and SNR decreases), P_D decreases not so dramatically and not synchronously, which is different from that of F-117A.

So, for a conventional aircraft like F-16 and a stealthy aircraft like F-117A, when they are close to a hostile radar, they perform almost the same from the perspective of detection probability. But when they get farther away from the radar, the difference becomes obvious; F-16 still keeps a high P_D value in a broad azimuth angle domain, which means it can be easily detected. But the P_D value of F-117A decreases fast in a broad angle domain, which means it gets undetected quickly.

The false alarm probability here is set to be $P_{fa} = 10^{-6}$. If we spend more time, we can draw a more complex figure for a specific target, where P_D varies with SNR, P_{fa} , and target's attitude angle, like figures that often appear in radar detection textbooks.

From Fig. 9 and the possible more complex figures, we can obtain very rich and relatively accurate information about a specific aircraft's stealth performance in front of threatening radars. This is the advantage of our method over other general detection models or basic RCS models.

Then we would like to discuss the instantaneous tracking probability, P_{track} , as mentioned in "Zeitz's Function" section.

The appendix of Zeitz (2005) gives the detailed derivation of P_{track} . It is a recursive expression and can be solved by recursive method. P_D is assumed to be a constant here; l and n are system constants.

$$z[n+1] = (1 - z[n-l])P_D(P_m)^l + z[n]$$

$$P_{track} = 1 - z[n]$$
(16)

Equations 4 and 5 can be used to calculate a specific target's P_{track} when P_D is obtained. We can directly use those discrete P_D values in this equation, so does P_m . Each P_{track} corresponds to the same azimuth angle as P_D .

Figure 10 is an example based on the data of Fig. 9. The detection distance is set to be a constant, R_0 . The radar system's constants are $n = 30$ and $l = 5$; if we want to know more results, R , n and l can be adjusted conveniently. Figure 10 shows that both aircrafts' P_{track} curves have nearly the same trend as their P_D curves in Fig. 9, and F-117A performs better almost in all directions, except in its leading edge's normal direction. When the detection distance increases, the P_{track} of F-117A decreases fast and synchronously in the whole angle domain just as curves in Fig. 9(a). And the P_{track} of F-16 decreases not so dramatically and not synchronously when the detection distance increases, just as curves in Fig. 9(b).

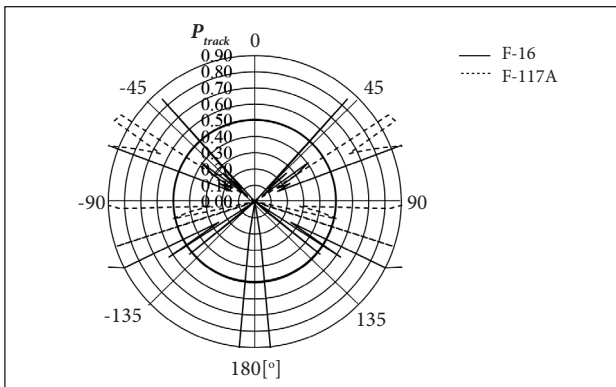


Figure 10. Target's instantaneous tracking probability in azimuth angle.

If we want to calculate the average tracking probability in a certain time interval, we just need to integrate the P_{track} values over the time interval and average the results, as shown in Eq. 7. Note that, in a specific combat situation, target's attitude angles may have different time periods of being presented to the radar, so the P_{track} values corresponding to each angle may be integrated with different time periods.

A CALCULATION EXAMPLE

A calculation example using the RCS data of X-21 is given in Fig. 11 to illustrate how detection and tracking probabilities vary with target's distance and azimuth angle in a combat situation.

We choose a simple but representative situation to demonstrate the calculation results. The target is flying from a longitudinal distance of $y_1 = 9.90 R_0$ towards the radar at a cross distance of $x_0 = 4 R_0$ (R_0 is a normalized distance). The azimuth angle between radar and target is $\theta_1 = 22^\circ$ when the target is at (x_0, y_1) , and y_i ($i = 2, 3, \dots, 69$) is chosen to be $9.42 R_0, 8.98 R_0, 8.58 R_0$ etc. to make sure that their corresponding azimuth angles are $\theta_2 = 23^\circ, \theta_3 = 24^\circ, \theta_4 = 25^\circ$, until $\theta_{69} = 90^\circ$. $P_{D,i}$ and $P_{track,i}$ are the detection and tracking probabilities at (x_0, y_i) ($i = 1, 2, \dots, 69$), and their curves are shown in Fig. 11. The peaks at about $y = 7.8 R_0$ and $y = 6.0 R_0$ correspond to the normal directions of the wing's leading edge and the horizontal tail's leading edge, respectively. When X-21 is far from the radar, its P_D and P_{track} are low, except the peaks. When it is close to the radar, its P_D and P_{track} become higher due to a larger RCS value and a larger SNR.

The average value of being tracked during its flying time can be calculated based on the discrete P_{track} values. As $\Delta y_i = y_{i+1} - y_i$ decreases with i , the integration time corresponding to each $P_{track,i}$ ($i = 1, 2, \dots, 69$) decreases with i , if the target has a constant velocity. The flight path is divided into 3 phases here for simplicity; each phase corresponds to a distance of $3.3 R_0$, and their average P_{track} values are 0.08, 0.11 and 0.68, respectively.

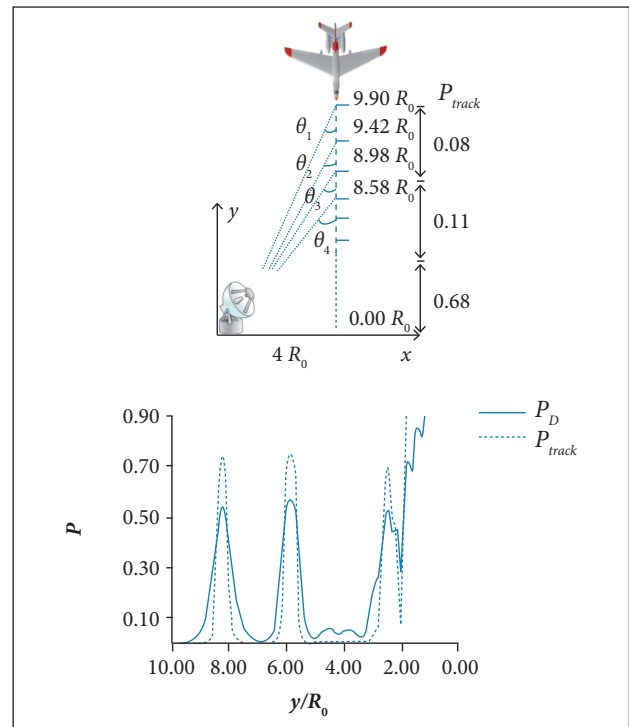


Figure 11. Target's P_D and P_{track} in a simple combat situation ($n = 30, l = 5, P_{fa} = 10^{-6}$).

CONCLUSIONS

The calculation of single pulse detection probability for RCS fluctuation targets has been analyzed and a new RCS model generation method has been proposed as the basis of the calculation. This method takes random factors like target's micro motions and air flow turbulence into account, so it conforms better to the reality. The RCS model can be directly used to calculate the detection probability of any specific aircraft at any attitude. Some typical aerial vehicles are

taken as examples to illustrate this method. The instantaneous probability of being tracked has also been introduced and it can be calculated if the detection probability is obtained. By this method, the single pulse detection probability and instantaneous probability of being tracked for a specific target can be calculated conveniently. Very rich information such as detection probability, false alarm probability, SNR, detection distance etc. can be obtained. Using this information, we can compare two different targets' stealth performance or optimize a target's flight path.

REFERENCES

- Bortoff SA (2000) Path planning for UAVs. Proceedings of the American Control Conference, American Automatic Control Council; Dayton, USA.
- David KB (2007) Radar system analysis and modeling (in Chinese, translated by Nanjing Institute of Electronic Technology). Beijing: Publishing House of Electronics Industry.
- Difanco JV, Rubin WL (1968) Radar detection. New Jersey: Prentice-Hall.
- Ding XD, Liu Y, Li WM (2008) Dynamic RCS and real-time based analysis of method of UAV route planning (in Chinese). Systems Engineering and Electronics 30(5):868-871.
- Dogan A (2003) Probabilistic approach in path planning for UAVs. Proceedings of the 2003 IEEE International Symposium on Intelligent Control; Houston, USA.
- Goerzen C, Mettler ZKB (2010) A survey of motion planning algorithms from the perspective of autonomous UAV guidance. J Intell Robot Syst 57(1-4):65-100. doi: 10.1007/s10846-009-9383-1
- Hebert JM (2001) Air vehicle path planning (PhD thesis). Wright-Patterson Air Force Base, Ohio: U.S. Air Force Institute of Technology.
- Inanc T, Muezzinoglu MK (2008) Framework for low-observable trajectory generation in presence of multiple radars. J Guid Control Dynam 31(6):1740-1750. doi: 10.2514/1.35287
- Johnston SL (1997) Target model pitfalls (illness, diagnosis, and prescription). IEEE T Aero Elec Sys 33(2): 715-720. doi: 10.1109/7.588498
- Kabamba PT, Meerkov SM, Zeitz FH (2006) Optimal path planning for unmanned combat aerial vehicles to defeat radar tracking. J Guid Control Dynam 29(2):279-289. doi: 10.2514/1.14303
- Kim BS, Bang H (2007) Optimal path planning for UAVs to reduce radar cross section. Int J Aeronautical & Space Sci 8(1):54-64. doi: 10.5139/IJASS.2007.8.1.054
- Liu HF, Chen SF, Zhang Y, Chen J (2012) Modelling radar tracking features and low observability motion planning for UCAV. Proceedings of the 4th International Conference on Intelligent Human-Machine System and Cybernetics; Nanchang, Jiangxi Province, China.
- Misovec K, Inanc T, Wohletz J, Murray RM (2003) Low-observable nonlinear trajectory generation for unmanned air vehicles. Proceedings of the 42nd IEEE Conference on Decision and Control, Maui, Hawaii, USA.
- Mo S, Huang J, Zheng Z, Liu W (2014) Stealth penetration path planning for stealth unmanned aerial vehicle based on improved rapidly-exploring-random-tree. Control Theory & Applications 31(3):375-385.
- Moore FW (2002) Radar cross-section reduction via route planning and intelligent control. IEEE T Contr Syst T 10(5):696-700. doi: 10.1109/TCST.2002.801879
- Paterson J (1999) Overview of low observable technology and its effects on combat aircraft survivability. J Aircraft 36(2):380-388. doi: 10.2514/2.2468
- Robinson MC (1992) Radar cross section models for limited aspect angle windows (Master's thesis). Montgomery: Air University.
- Scholefield PHR (1967) Statistical aspects of ideal radar targets. Proceedings of the IEEE 55(4):587-589. doi: 10.1109/PROC.1967.5610
- Shnidman DA (1995) Radar detection probabilities and their calculation. IEEE T Aero Elec Sys 31(3):928-950. doi: 10.1109/7.395246
- Shnidman DA (2005) Radar detection in clutter. IEEE T Aero Elec Sys 41(3):1056-1067. doi: 10.1109/TAES.2005.1541450
- Swerling P (1960) Probability of detection for fluctuating targets. IRE Transactions on Information Theory 6(2):269-308. doi: 10.1109/TIT.1960.1057561
- Wu SJ, Zheng Z, Cai KY (2011) Real-time path planning for unmanned aerial vehicles using behavior coordination and virtual goal (in Chinese). Control Theory & Applications 28(1):131-136.
- Xu C, Duan H, Liu F (2010) Chaotic artificial bee colony approach to uninhabited combat air vehicle (UCAV) path planning. Aerosp Sci Technol 14(8):535-541. doi: 10.1016/j.ast.2010.04.008
- Zeitz FH (2005) UCAV path planning in the presence of radar-guided surface-to-air missile threats (PhD thesis). Ann Arbor: University of Michigan.